AN EXPERIMENTAL AND THEORETICAL INVESTIGATION OF CREEP BUCKLING

H. OHYA

Ishikawajima-Harima Heavy Industries Co., Ltd., Research Institute, 1–15, Toyosu 3-Chome, Koto-ku, Tokyo, 135–91, Japan

SUMMARY

Creep buckling is one of the failure modes which must be taken into consideration for the design of structures exposed to elevated temperatures. And, rules are provided in ASME Boiler and Pressure Vessel Code Case 1592 to prevent the creep buckling. However, methods of analysis are not provided in Code Case, and selecting the methods of analysis is left to owners and manufacturers.

The purpose of the present paper is to investigate creep buckling phenomena and the methods of analysis. Creep buckling experiments were performed on aluminum alloy 2024-T4 cylindrical shells having radius to thickness ratios of 16, 25, 50 and 80, in single, double and triple step axial compression at 250 ℃. It was observed that buckling occurred at one of the edges and the buckling mode depended on the radius to thickness ratio and also on the applied stress level. Thicker cylinders buckled in axisymmetric mode. Thinner ones under higher applied stress levels buckled in the asymmetric mode, whereas they under lower applied stress levels buckled in the axisymmetric mode. Creep buckling times were obtained from end shortening record of the cylinders.

Experimental results were compared with theoretical values obtained by the following two methods. One is a simplified method to estimate buckling times, proposed by Gerard *et al.*, Papirno *et al.* and others. The method is based on the fact that the creep buckling solutions are analogous to those of plastic buckling under a certain assumption. It was found that the buckling times could be reasonably estimated by this simplified method. The other is a finite element computer program for axisymmetric thin shells. This program is based on the incremental theory and can treat thermoelastoplastic creep analysis of axisymmetric thin shells with large deflection. Creep deformation behavior of cylindrical shells under axial compression and buckling times were calculated by the program and the effects of plasticity on buckling times were also investigated.

A cumulative damage rule for creep buckling,

$$\sum_i (t/t_{cr})_i = 1 \ ,$$

was assumed to apply the simplified method mentioned above to changing stress/temperature conditions. The validity of this rule was investigated by various theoretical methods and experimental results. At first, the solutions of the creep buckling analysis for columns and cylindrical shells by Hoff were used to investigate the validity of this rule. It was confirmed that this rule was strictly valid under conditions that elasticity was neglected and secondary creep law was assumed. Next, the simplified method and the finite element computer program both of which were mentioned above were used. It was shown that this rule was reasonable when the difference between consecutive stress levels was not so large. Lastly, creep buckling experiments were performed on cylindrical shells in double and triple step axial compression and the validity of this rule was also investigated.

1. Introduction

Creep buckling is one of the failure modes which must te taken into consideration in the design of structures exposed to high temperatures. Rules are provided in ASME Boiler and Pressure Vessel Code Case 1592 to prevent creep buckling. However, methods for analysis are not provided in the Code Case.

There are several experimental and theoretical studies performed on creep buckling of cylindrical shells under axial compression [1] ∿ [7], however, comparison of experimental results with theoretical ones does not seem to be sufficient.

Therefore, experiments and theoretical analyses were performed on creep buckling of cylindrical sheels under axial compression to investigate creep buckling phenomena and methods for analysis. Further, a method for easier evaluation of creep buckling under varying stress/temperature conditions was established and validity thereof was examined by several methods.

2. Experiments

Creep buckling experiments were performed on cylindrical shells under axial compression.

2.1 Experimental program

The material used in this experiment was aluminum alloy 2024-T4. In order to investigate the properties of the material, short time tensile tests and tensile creep tests, both under 250°C, were performed. Stress-strain curves obtained are approximated by a bilinear representation.

$$E = 6920 \text{ kg/mm}^2, \quad \sigma_y = 25.7 \text{ kg/mm}^2, \quad H' = 113 \text{ kg/mm}^2$$

Also, the creep property of the material is represented by the following equation.

$$\varepsilon^c = 2.59 \times 10^{-11} \sigma^{6.49} t + 1.39 \times 10^{-6} \sigma^{2.1} t^{0.274} \qquad (1)$$

where ε^c : (mm/mm), σ : (kg/mm^2), t : (hr).

Cylindrical test specimens were manufactured from the commercial aluminum alloy rods by turning in a lathe.

Fig. 1 shows the test specimen. Four kinds of test specimens with identical length of 50 mm, identical radius R of 16 mm and different thickness h, namely, R/h = 16, 25, 50 and 80, were manufactured. Dimensional check was made after manufacturing test specimens.

The testing equipment consists of a loading device, an electric furnace, a temperature measuring instrument, a temperature control device and an end shortening measuring device. The boundary condition of the test specimen was plane compression. End shortening of the test specimen was detected by two dial gauges, and was recorded as a function of time on a pen recorder. Test temperature was 250°C and measured by two thermocouples.

2.2 Experimental results

Fig. 2 shows some typical end shortening vs. time curves recorded by pen recorder.

All the results of experiments are summarized in Table I. Buckling time t_{cr} was defined as the time when the end shortening rate approached infinity. It is seen in Table I that buckling mode is classified into two forms, namely, axisymmetric one and asymmetric one.

Although the number of circumferential waves obtained was scattered in some extent, the following conclusions can be drawn with regard to the relationship between thickness of

cylinder, applied stress level and buckling mode. Thicker cylinders buckled in axisymmetric mode. Thinner ones under higher applied stress levels buckled in asymmetric mode, whereas under lower applied stress levels, they buckled in axisymmetric mode. As for the number of circumferential waves in the asymmetric mode, the thinner the cylinder was, the more was the number of circumferential waves under the same stress level. Also, buckling occurred at one of the edges regardless of buckling mode, which indicates that the edge effect is important.

In Fig. 2, the end shortening vs. time curves appear to be different for cylinders of different wall thickness. And, the end shortening at buckling becomes smaller as the wall thickness becomes thinnner.

3. Theoretical analyses

Creep buckling analyses using existent simplified methods and a finite element computer program made by the author and comparison with experimental results are discussed herein.

3.1 Simplified methods of creep buckling

3.1.1 Method for analysis

A perfect cylindrical shell with no initial imperfection under axial compression is considered in this discussion.

The mechanical properties are considered to change as a function of time, and a time dependent problem is replaced by an equivalent time independent problem.

A long cylindrical shell, length and boundary condition of which do not give effects on buckling, is considered herein.

The following four equations have been proposed for creep buckling calculation.

∘ Papirno & Goldman's method [4]

$$\sigma = C\eta E \frac{h}{R} \tag{2}$$

where C : buckling coefficient, η : plastic reduction factor

∘ Griffin's method [7]

$$\sigma = \left[\frac{E_T E_S}{3(1 - \upsilon^2)} \right]^{1/2} \frac{h}{R} \tag{3}$$

where E_T : tangent modulus, E_S : secant modulus, υ : Poisson's ratio

∘ Samuelson's method [2]

$$\sigma = K \left(E_T E_S \right)^{1/2} \frac{h}{R} \tag{4}$$

where K : buckling constant

∘ Gerard & Gilbert's method [1]

$$\sigma = 0.6 E_S \frac{h}{R} \tag{5}$$

Creep buckling occurs when η, υ, E_T and E_S change as a function of time and satisfy eqs. (2) through (5).

3.1.2 Results of analyses

Creep buckling times were calculated using above four equations and compared with experimental results.

Fig. 3 shows a comparision of calculated values and experimental results (R/h = 16) by

plotting applied stress on the ordinate and buckling time on the abscissa. Fig. 4 shows a comparison of calculated values (Papirno & Goldman's method) and experimental results by plotting buckling time obtained by experiments on the ordinate and calculated buckling times on the abscissa. In Fig. 4, △ mark indicates axisymmetric buckling mode observed in experiments and ○ mark indicates asymmetric buckling mode.

Based on comparison of experimental results and theoretical values, it is considered that the simplified methods provide reasonable results whether buckling modes are axisymmetric or asymmetric.

3.2 Finite element method

Analyses of creep buckling using a finite element computer program for axisymmetric thin shells is discussed herein. This program is based on the incremental theory and can treat thermoelastoplastic creep analysis of axisymmetric thin shells with large deflection.

3.2.1 Theory

An axisymmetric shell is idealized as an assembly of conical frustra elements.

(1) Strain - displacement relation

The meridian and circumferential strains ε_s and ε_θ at distance z from the middle surface of the shell are expressed by

$$\varepsilon_s = e_s - zk_s \quad , \quad \varepsilon_\theta = e_\theta - zk_\theta \tag{6}$$

where e_s, e_θ and k_s, k_θ indicate strains and curvature changes of the middle surface, respectively.

The following equations are used for strain - displacement relation, taking into account of geometric nonlinearity:

$$e_s = \frac{du}{ds} + \frac{1}{2}\left(\frac{dw}{ds}\right)^{1/2} \quad , \quad e_\theta = (u \sin\phi + w \cos\phi)/r$$
$$k_s = \frac{d^2w}{ds^2} \quad , \quad k_\theta = \frac{\sin\phi}{r}\frac{dw}{ds} \tag{7}$$

(2) Constitutive equations

Total strain increment is decomposed into increments of elastic strain $\{\varepsilon^e\}$, thermal strain $\{\varepsilon^\theta\}$, plastic strain $\{\varepsilon P\}$ and creep strain $\{\varepsilon^c\}$.

$$\{\Delta\varepsilon\} = \{\Delta\varepsilon^e\} + \{\Delta\varepsilon^\theta\} + \{\Delta\varepsilon P\} + \{\Delta\varepsilon^c\} \tag{8}$$

where $\{\varepsilon\} = [\varepsilon_s \ \varepsilon_\theta]^T$, Δ: increment

Each strain increment is calculated taking into consideration temperature dependent material properties.

Plastic strain increment is derived using von Mises's yield criterion and its associated flow rule. Both isotropic and kinematic hardening rules are considered.

According to Cry & Teter [8], and Rashid [9], creep strain increment is given by the following equation.

$$\{\Delta\varepsilon^c\} = [C^c]\{\Delta\sigma\} + \{\Delta\hat{\varepsilon}^c\}\} \tag{9}$$

where $\{\sigma\} = [\sigma_s \ \sigma_\theta]^T$

Stress increment - strain increment relation is obtained by these strain increments.

(3) Equilibrium equation

Using the principle of virtual work, the following equilibrium equation is obtained.

$$[K] \{\Delta d\} = \{\Delta F + \Delta F\theta + \Delta F^c\} + \{-R + F\} \quad (10)$$

where $[K]$: stiffness matrix

$\{\Delta d\}$: incremental nodal displacement

$\{\Delta F\}$: incremental equivalent nodal forces

$\{\Delta F\theta\}$: incremental equivalent nodal forces due to temperature change

$\{\Delta F^c\}$: incremental equivalent nodal forces due to creep strain

$\{R\}$: reaction nodal forces calculated from initial stresses

$\{F\}$: total equivalent nodal forces applied to the system at the end of the preceding step

Eq. (10) is the linear simultaneous equatations for $\{\Delta d\}$ and can be solved by the Gauss elimination method.

3.2.2 Results of analyses

The computer program has been prepared based on the theory described in para. 3.2.1. Figs. 5 and 6 show the examples of end shortening vs. time curves obtained using this program, together with experimental results. Because of the symmetrical load and geometry of the shell, half portion of the cylinder is analyzed with 17 elements. The coordinate system of this cylinder is shown in Fig. 1. The radial displacement is fixed and the rotation is set free at the edge of the cylinder. In the creep analysis, strain hardening rule is adopted.

Although the program used herein takes into consideration axisymmetric deformation only, the calculated results agree with the experimental ones within adequate range whether the experimental buckling modes are axisymmetric or not, which is explained by the experimental results by Samuelson [2] [3] showing that axisymmetric deformation is observed until just prior to buckling even though it occurs in asymmetric mode.

Figs. 7 and 8 show time history of deflection and distribution of plastic range obtained by calculation in case of $R/h = 16$, $\sigma = 18$ kg/mm^2. Deflection pattern indicates a peak deflection near the end part where radial displacement is constrained, which becomes sharply large as it approaches to buckling time. In Fig. 8, it is observed that the plastic range first appears inside just before the buckling time arrives, and then the plastic range gradually spreads. However, even at the time of buckling, the plastic range is observed only at the part where the peak deflection appears, and it is considered that effect of plasticity on creep buckling is not so large as far as author's calculation is concerned.

4. Cumulative damage rule for creep buckling

The simplified method described in para. 3.1 easily gives creep buckling time under constant stress and temperature conditions. A cumulative damage rule to apply this simplified method to varying stress/temperature conditions is discussed herein.

A life expectancy hypothesis for estimating life of aircraft was proposed by Gerard [10]. In the present paper, Gerard's hypothesis is applied to creep buckling, and a cumulative damage rule as defined by the following equation is assumed.

$$\sum_i \frac{t_i}{t_{cri}} = 1 \quad (11)$$

where t_i : time duration of the load condition i

t_{cri} : creep buckling time under the load condition i

Validity of eq. (11) is investigated by several methods in the following paragraph.

4.1 Analytical solution

Validity of eq. (11) is examined by the analytical solutions for simple models made by Odquvist and Hoff.

Instantaneous deformation is neglected herein.

4.1.1 Rigid column model

A model of straight rigid column, hinged at the lower end and supported sideways at the upper end by a spring, as shown in Fig. 9, is considered herein. The spring is assumed to follow secondary creep law.

In this model, if elastic deformation is ignored, angle ϕ at time t is given by the following equation [11].

$$\frac{1}{\phi^{n-1}} = \frac{1}{\phi_0^{n-1}} - \frac{(n-1)k/L\ P^n}{1 - P/P_E}\ t \tag{12}$$

where n : creep index (>1), P : applied load,

P_E : elastic buckling load

Creep buckling time is given by putting $\phi \to \infty$ in eq. (12).

Then, consider the case where loads P_1, P_2 and P_3 are applied consecutively for a period of t_1, t_2 and t_3 respectively, until the time when buckling occurs. Angle ϕ_1, after load P_1 is applied for a period of t_1 is given by eq. (12) as follows.

$$\phi_1 = \left[\phi_0^{1-n} - \frac{(n-1)k/L\ P_1^n}{1 - P_1/P_E} \right]^{\frac{1}{1-n}} = \phi_0 \left(1 - \frac{t_1}{t_{cr1}}\right)^{\frac{1}{1-n}} \tag{13}$$

Angle ϕ_2 after load P_2 is applied for a period of t_2 with ϕ_1 being an initial condition is given by eq. (12) as follows.

$$\phi_2 = \left[\phi_1^{1-n} - \frac{(n-1)k/L\ P_2^n}{1 - P_2/P_E} \right]^{\frac{1}{1-n}} = \phi_0 \left(1 - \frac{t_1}{t_{cr1}} - \frac{t_2}{t_{cr2}}\right)^{\frac{1}{1-n}} \tag{14}$$

Then, making ϕ_2 an initial condition, and assuming buckling occurs after load P_3 is applied for a period of t_3, eq. (12) will be solved as follows:

$$0 = \frac{1}{\phi_2^{n-1}} - \frac{(n-1)k/L\ P_3^n}{1 - P_3/P_E}\ t_3 = \phi_2^{1-n} - \phi_0^{1-n} \frac{t_3}{t_{cr3}}$$

$$= \phi_0^{1-n} \left(1 - \frac{t_1}{t_{cr1}} - \frac{t_2}{t_{cr2}} - \frac{t_3}{t_{cr3}}\right) \tag{15}$$

Based on eq. (15), the following equation is obtained.

$$\sum_{i=1}^{3} \frac{t_i}{t_{cri}} = 1 \tag{16}$$

This result can be extended to the case of i = n.
Consequently, eq. (11) is proven to be valid generally.

4.1.2 Cylindrical shell under axial compression

A cylindrical shell under axial compression is discussed herein. An equation for secondary creep is used as a creep law, and the case of n = 3 is investigated in the following.

When a cylindrical shell having an initial amplitude x_0 at time t = 0 is put under axial compressive load and deformed by creep, the relationship between amplitude x and time t, and buckling time are given by the following equatations [5].

$$t = 0.294\ t_E\ \ell n\ \frac{x^2(1.18 + x_0^2)}{x_0^2(1.18 + x^2)} \tag{17}$$

$$t_{cr} = 0.294\ t_E\ \ell n\ \frac{1.18 + x_0^2}{x_0^2} \tag{18}$$

where t_E : Euler time

From eqs. (17) and (18), eq. (11) is proven to be valid by the same procedure as in the case of the rigid column model.

4.2 Simplified method

Validity of eq. (11) is examined by the simplified method on a cylindrical shell under axial compression as described in para. 3.1.

A cylindrical shell under triple step axial compression is discussed herein. Eq. (5) is used as a simplified method. Calculation is performed on a test specimen of R/h = 80 as described in para. 2.1. The calculation was performed for the case of σ = 14 and 12 kg/mm^2 in triple step. The results of calculation are shown in Table II.

It is observed in Table II that reasonable results are obtained even in case of triple stepped loading.

4.3 Finite element method

A cylindrical shell under double step axial compression is discussed herein using the finite element computer program as described in para. 3.2. The calculated model is the same one as investigated in para. 4.2. The results of calculation are shown in Table III.

It is observed in Table III that the use-fraction sum will be above or below 1.0 depending on loading order, and the effect of relative relationship between σ_1 and σ_2 on the use-fration sum is recognized. That is, when σ_1 and σ_2 are close each other, the use-fraction sum is close to 1.0 and when σ_1 and σ_2 differ considerably each other, the use-fraction sum deviates from 1.0. As investigated in para. 4.1, eq. (11) is valid strictly when instantaneous deformation is neglected. When there is a difference between σ_1 and σ_2, instantaneous deformation during changing from σ_1 to σ_2 can not be neglected, which is considered to be the reason for deviation of the use-fraction sum from 1.0. However, eq. (11) is considered to be reasonable within practical stress range.

4.4 Experiments

Validity of eq. (11) is investigated by performing experiments on cylindrical shells under double and triple step axial compression using the testing equipment described in para.

2.1. Material and temperature are the same as those described in para. 2.1, and the experiments were performed on test specimen of R/h = 80. Tests were performed in the cases where σ = 12 and 14 kg/mm^2 applied in double step and triple step. The summary of experimental results is shown in Tables IV and V.

Scatter of the use-fraction sum is large in case of double stepped loading. One of the reasons for this may be a boundary condition of experiment. That is, the boundary condition of this experiment is plane compression applied to a test specimen which is placed between the jigs, but it may change when the loading is changed. Since buckling occurs at one of the edges, the effect of boundary condition on creep buckling is significant, and the change in boundary condition during loading change is believed to give a significant effect on buckling time.

As the experiment under triple stepped loading was performed on only one test specimen, no definitive conclusion can be derived, however, the results obtained appear to be reasonable.

4.5 Discussion

Validity of the cumulative damage rule for creep buckling represented by eq. (11) was investigated by two analytical solutions, a simplified method, a finite element method and experiments. The experimental results scatter to a great extent so that the further experiments should be carried out, however, the calculated results appear to be reasonable and evaluation of creep buckling can be done within practical stress range using eq. (11).

When eq. (11) is applied to evaluation of creep buckling, the denominator t_{cri} can be obtained by appropriate methods which are justified in calculating creep buckling time under constant stress and temperature conditions, for example, the simplified methods as described in para. 3.1.

Acknowledgement

This study was performed as a part of National Research and Development Program "Research and Development of Direct Reduction Steelmaking Process by Using High Temperature Reducing Gas" sponsored by Agency of Industrial Science and Technology, Ministry of International Trade and Industry.

The author expresses sincere thanks for guidance provided by the members of the High Temperature Heat Exchanger Strength Special Committee - Structural Analysis Committee (Chairman, Prof. Udoguchi, Chief, Prof. Yamada) under Engineering Research Association of Nuclear Steelmaking.

References

[1] Gerard, G. & Gilbert, A.C., "A Critical Strain Approach to Creep Buckling of Plates and Shells", J. Aero. Sci., Vol. 25, No. 7, P. 429, (1958).

[2] Samuelson, A., "An Experimental Investigation of Creep Buckling of Circular Cylindrical Shells", Aeronautical Research Institute of Sweden (FFA), Report No. 98, (1964).

[3] Samuelson, L.A., "Experimental Investigation of Creep Buckling of Circular Cylindrical Shells under Axial Compression and Bending", J. Engineering for Industry, Vol. 90, P. 589, (1968).

[4] Papirno, R. & Goldman, R., "Experimental Creep Buckling of Aluminum Cylinders in Axial Compression", Experimental Mechanics, Vol. 9, No. 8, P. 356, (1969).

[5] Hoff, N.J., "Axially Symmetric Creep Buckling of Circular Cylindrical Shells in Axial compression", Trans. ASME Ser. E, Vol. 90, P. 530, (1968).

[6] Samuelson, L.A., "Creep Buckling of a Circular Cylindrical Shell", AIAA, Vol. 7, No. 1, P. 42, (1969).

[7] Griffin, D.S., "Inelastic and Creep Buckling of Circular Cylinders Due to Axial Compression, Bending, and Twisting", ASME Paper 74-PVP-46, (1974).

[8] Cry, N.A. & Teter, R. D., "Finite Element Elastic-Plastic-Creep Analysis of Two-Dimensional Continuum with Temperature Dependent Material Properties", Computer & Structures, Vol. 3, P. 849, (1963).

[9] Rashid, Y. R., "Analysis of Multiaxial Flow under Variable Load and Temperature", Creep and Fatigue in Elevated Temperature Applications, C183/73, (1973).

[10] Gerard, G., "Life Expectancy of Aircraft under Thermal Flight Conditions", J. Aeronautical Sciences, Vol. 21, No. 10, P. 675, (1954).

[11] Odqvist, F. K. G. & Hult, J., Kriechfestigkeit metallischer Werkstoffe, (1962), Springer.

Table II Creep Buckling of Cylinders under Triple Step Axial Compression (Simplified Method)

σ_1 (kg/mm^2)	t_1 (hr)	σ_2 (kg/mm^2)	t_2 (hr)	σ_3 (kg/mm^2)	t_3 (hr)	$\sum_{i=1}^{3} \frac{t_i}{t_{cri}}$
14	1	12	3	14	2.11	0.981
12	2.5	14	1	12	7.24	1.015
12	3	14	1	12	6.76	1.016

Table I Results of Cylinder Creep Buckling Tests

No.	R/h	σ (kg/mm^2)	Mode	No. of circum-ferential waves	t_{cr} (hr)
1	16	14	Axi	0	33.3
2	16	14	"	0	27.6
3	16	15	"	0	13.6
4	16	16	"	0	9.90
5	16	18	"	0	6.95
6	25	14	"	0	27.6
7	25	16	"	0	5.54
8	25	16	"	0	4.49
9	25	18	"	0	4.66
10	25	18	"	0	0.837
11	50	6.2	"	0	710
12	50	10	"	0	70.7
13	50	10	Asym	4	81.3
14	50	12	"	*	30.4
15	50	14	"	3	7.08
16	50	14	"	4	14.2
17	50	16	"	4	1.33
18	80	10	"	6	30.3
19	80	10	"	*	39.2
20	80	12	"	6	10.6
21	80	12	"	6	13.2
22	80	12	"	*	7.68
23	80	14	"	6	2.31
24	80	14	"	6	2.07
25	80	15	"	6	0.108
26	80	16	"	7	0.132
27	80	16	"	7	0.0749
28	80	16	"	6	0.378
29	80	16	"	7	0.0967
30	80	16	"	6	0.263
31	80	16	"	6	0.144

* Number of circumferential waves is not known.

Table III Creep Buckling of Cylinders under Double Step Axial Compression (Finite Element Method)

σ_1 (kg/mm^2)	t_1 (hr)	σ_2 (kg/mm^2)	t_2 (hr)	$\sum_{i=1}^{2} \frac{t_i}{t_{cri}}$
12	4	14	3.10	0.984
12	8	14	1.76	0.973
14	1	12	10.87	1.009
14	2.5	12	6.37	1.021
6	600	12	8.69	0.959
6	1000	12	5.40	0.944
12	4	6	1335.3	1.028
12	8	6	844.6	1.045

Table IV Creep Buckling of Cylinders under Double Step Axial Compression (Experimental Results)

σ_1 (kg/mm^2)	t_1 (hr)	σ_2 (kg/mm^2)	t_2 (hr)	t_{cr} (hr)	$\sum_{i=1}^{2} \frac{t_i}{t_{cri}}$
14	1	12	12.4	13.4	1.638
14	1	12	16.5	17.5	2.028
14	1	12	18.5	19.5	2.219
12	4	14	1.02	5.02	0.847
12	4	14	0.792	4.79	0.743
12	4	14	2.72	6.72	1.621

Table V. Creep Buckling of Cylinders under Triple Step Axial Compression (Experimental Results)

σ_1 (kg/mm^2)	t_1 (hr)	σ_2 (kg/mm^2)	t_2 (hr)	σ_3 (kg/mm^2)	t_3 (hr)	t_{cr} (hr)	$\sum_{i=1}^{3} \frac{t_i}{t_{cri}}$
14	1	12	3	14	0.399	4.40	0.925

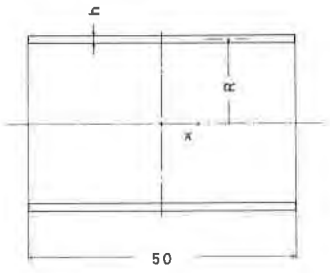

Fig. 1 Test specimen

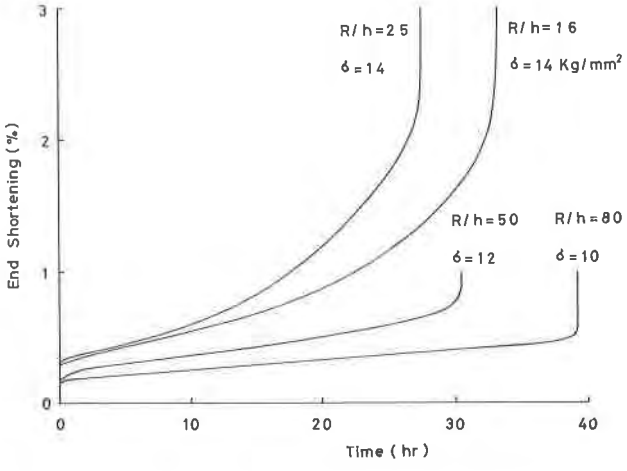

Fig. 2 End shortening - time curves

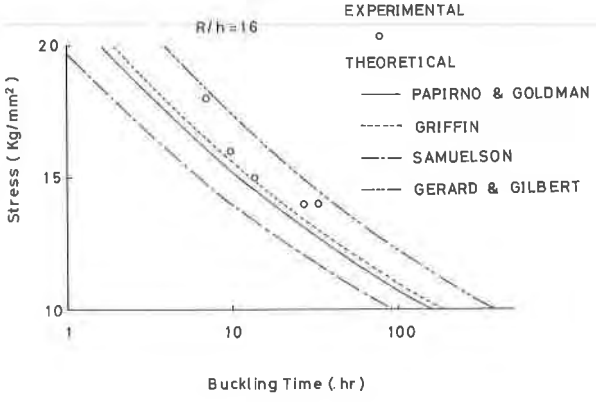

Fig. 3 Stress - buckling time (R/h = 16)

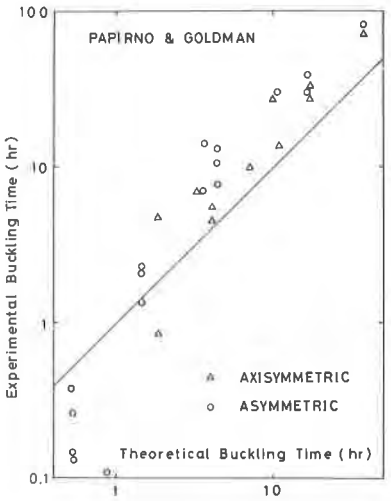

Fig. 4 Correlation of experimental creep buckling times and theory

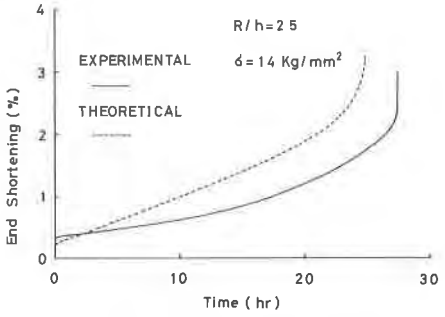

Fig. 5 End shortening - time curves

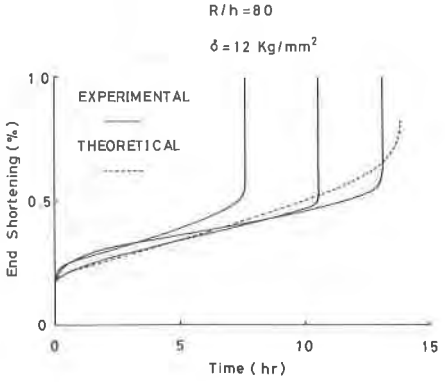

Fig. 6 End shortening - time curves

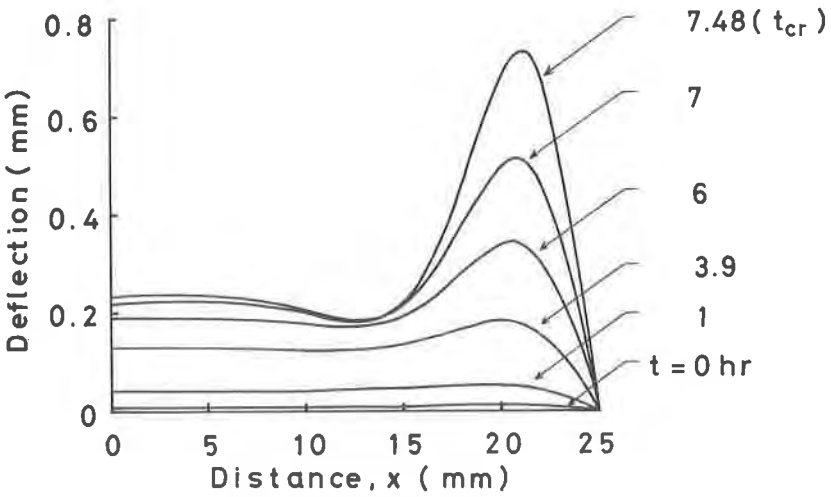

Fig. 7 Distribution of deflection (R/h = 16, σ = 18 kg/mm^2)

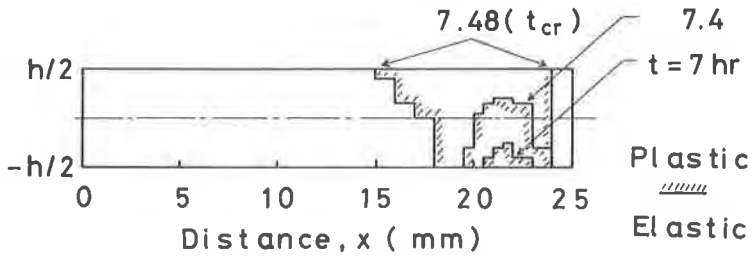

Fig. 8 Distribution of plastic range (R/h = 16, σ = 18 kg/mm^2)

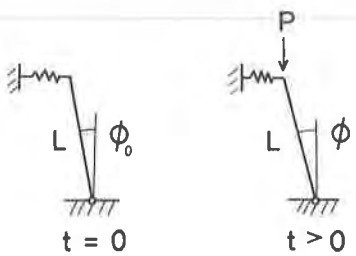

Fig. 9 Rigid column model